PARP inhibitors and radiation potentiate liver cell death in vitro. Do hepatocellular carcinomas have an achilles' heel?

Laetitia Gerossier, Anaëlle Dubois, Alexia Paturel, Nadim Fares, Damien Cohen, Philippe Merle, Joel Lachuer, Anne Wierinckx, Pierre Saintigny, Brigitte Bancel, et al.

PARP inhibitors and radiation potentiate liver cell death *in vitro*. Do hepatocellular carcinomas have an Achilles' heel?

Short title: PARP inhibitors and radiotherapy for HCC treatment

Laetitia Gerossier[1†], Anaëlle Dubois[1†], Alexia Paturel[1], Nadim Fares[1**], Damien Cohen[1], Phillippe Merle[1,2], Joel Lachuer[1,3], Anne Wierinckx[1,3], Pierre Saintigny[1,4], Brigitte Bancel[5], Janick Selves[6], Anne Schnitzler[7], Bérengère Ouine[8], Aurélie Cartier[8], Leanne de Koning[8], Vincent Puard[8], Ivan Bieche[7], Hector Hernandez-Vargas[1], Janet Hall[1], Isabelle Chemin[1*].

1. Univ Lyon, Université Claude Bernard Lyon 1, INSERM, CNRS, Centre Léon Bérard, Centre de Recherche en Cancérologie de Lyon, Lyon, 69008, France.
2. Department of Hepatology, Groupement Hospitalier Nord, Hospices Civils de Lyon, Lyon, 69000 France
3. ProfileXpert, SFR-Est, CNRS UMR-S3453, INSERM US7, Lyon Cedex 08, F-69373, France
4. Department of Medical Oncology, Centre Léon Bérard, Lyon, France
5. Service d'Anatomopathologie, Groupement Hospitalier Est, Hospices Civils de Lyon, Lyon, 69000, France
6. Anatomie et cytologie pathologiques Pôle IUC Oncopole CHU Institut Universitaire du Cancer de Toulouse - Oncopole, Toulouse, F- 31059, France
7. Department of Genetics, Institut Curie, PSL Research University, Paris, F-75005, France
8. Department of Translational Research, Institut Curie, PSL Research University, Paris, F-75005, France

* To whom correspondence should be addressed. Tel: +33 472681973; Fax: +33 472681971 Email: Isabelle.chemin@inserm.fr

** present address: Department of Digestive Oncology Rangueil Universitary Hospital, Hopitaux de Toulouse, Toulouse France.

† These authors contributed equally to this work.

Keywords

Liver cancer, hepatitis B virus (HBV) X protein, gammaH2AX, DNA damage, SMC5/6, Talazoparib, Veliparib.

Conflict of Interest Statement

None declared.

Funding

This work was supported by funding from La Ligue Nationale Contre le Cancer, the ANRS (grant number 12357 to D.C.) and La Ligue Contre le Cancer Rhone Alpes.

Abstract

Background

A promising avenue for cancer treatment is exacerbating the deregulation of the DNA repair machinery that would normally protect the genome. To address the applicability of poly(ADP-ribose) polymerase (PARP) inhibitors (PARPi) combined with radiotherapy for the treatment of hepatocellular carcinoma (HCC) two approaches were used: firstly, the *in vitro* sensitivity to the PARPi Veliparib and Talazoparib +/- radiation exposure was determined in liver cell lines and the impact of the HBV X protein (HBx) that deregulates cellular DNA damage repair via SMC5/6 degradation was investigated. Secondly, PARP expression profiles and DNA damage levels using the surrogate marker gammaH2AX were assessed in a panel of control liver *vs* HCC tissues.

Methods

Cell cytotoxicity was measured by clonogenic survival or relative cell growth and the DNA damage response using immunological-based techniques in Hep3B, PLC/PRF/5, HepG2- and HepaRG-derived models. Transcriptome changes due to HBx expression *vs* SMC6 loss were assessed by RNA sequencing in HepaRG-derived models. PARP and PARG transcripts (qPCR) and PARP1, H2AX and gammaH2AX protein levels (RPPA) were compared in control liver *vs* HBV-, HCV-, alcohol- and non-alcoholic steatohepatitis-associated HCC (tumor/peritumor) tissues.

Results

PARPi cytotoxicity was significantly enhanced when combined with X-rays (2Gy) with Talazoparib having a greater impact than Veliparib in most *in vitro* models. HBx expression significantly lowered survival, probably driven by SMC5/6 loss based on the transcriptome analysis and higher DNA damage levels. PARP1 and PARP2 transcript levels were significantly higher in tumor than peritumor and control tissues. The HBV/HCV/alcohol-associated tumor tissues studied had reduced H2AX but higher gammaH2AX protein levels compared to peritumor and control tissues providing evidence of increased DNA damage during liver disease progression.

Conclusions

These proof-of-concept experiments support PARPi alone or combined with radiotherapy for HCC treatment, particularly for HBV-associated tumors, that warrant further investigation.

Graphical Abstract

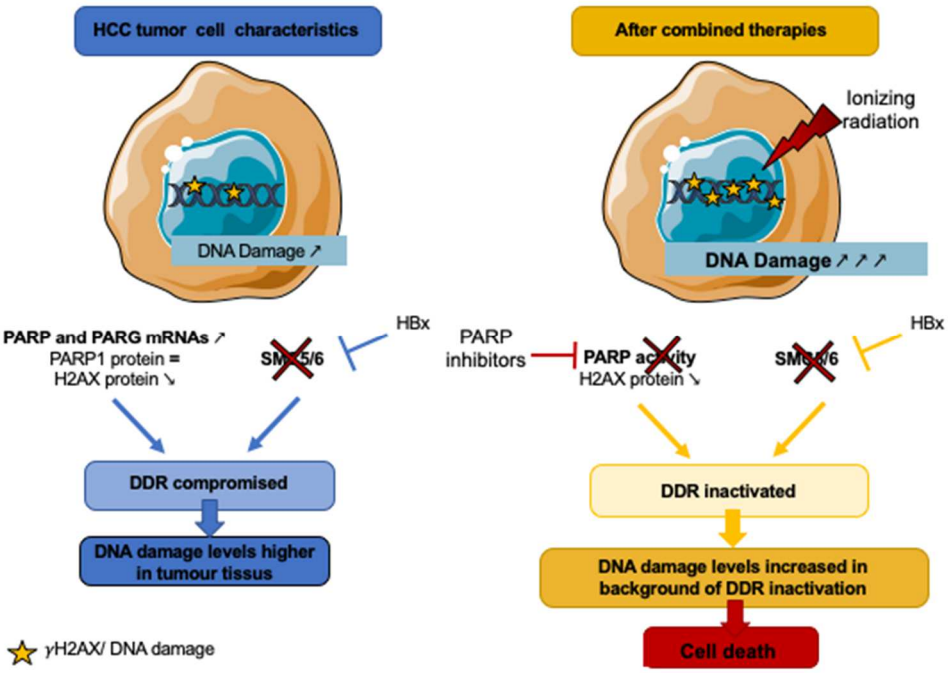

List of abbreviations

HCC (Hepatocellular carcinoma); RT (radiotherapy); HBV (hepatitis B virus); SBRT (sterotactic body RT); PARP (poly(ADP-ribose) polymerases); PARPi (PARP inhibitors); IR (ionizing radiation); HBV (hepatitis B virus); HBx (hepatitis B virus X protein); SMC5/6 (structural maintenance of chromosomes complex 5 and 6); HR (homologous recombination); DSBs (double strand breaks); PARG (poly(ADP-ribose) glycohydrolase); gammaH2AX (serine 139 phosphorylated Histone H2AX); PT (peritumor); T (tumor); HepaRG TR (HepaRG cells containing a plasmid with the tetracycline promotor); HepaRG TRX (HepaRG cells expressing the HBx protein under a tetracycline inducible promotor); HepaRG TRX sh-scramble (cells expressing an in-efficient shRNA construct in a lentiviral GFP vector); HepaRG TRX sh-SMC6 (cells expressing a 29mer shRNA construct targeting the SMC6 transcript); HU (hydroxyurea); DAPI (4,6-diamidino-2-phenylindole); AU (arbitrary units); D_{37} (mean lethal dose); RPPA (Reverse Phase Protein Array); FPKM (Fragments Per Kilobases of exon per Million mapped reads); DDR (DNA damage response).

Introduction

Over 90% of primary liver cancers are hepatocellular carcinomas (HCC) and an often too late diagnosis and few treatment options can explain their poor prognosis. Treatment with systemic chemotherapy are ineffective in HCC and many of the main oncogenic HCC drivers, such as the TERT promoter, TP53 and CTNNB1 [1], have not proven to be targetable. In contrast to many other cancer sites, ionising external beam radiotherapy (RT) has not been widely used in HCC management outside the palliative setting [2]. However, with recent technological advances in radiation delivery, hypofractionated sterotactic body RT (SBRT) used as a monotherapy or in combination with other liver-directed therapies (reviewed in [2, 3]) or with radiosensitising drugs such as poly(ADP-ribose) polymerases (PARP) inhibitors (PARPi) [4] could provide promising local control and support their use for HCC.

In order to explore the potential of PARPi for HCC treatment, we have expanded an *in vitro* pilot study [5] showing that concomitant Veliparib and ionizing radiation (IR) treatment lowered liver cell survival to assess a second PARPi Talazoparib and the impact of the expression of hepatitis B virus (HBV) encoded X (HBx) protein on this response. HBx degrades the cell's structural maintenance of chromosomes complex 5 and 6 (SMC5/6) to allow the completion of the HBV lifecycle [6]. The SMC5/6 complex participates in homologous recombination (HR), one of two major DNA double strand break (DSB) repair pathways and promotes sister-chromatid HR during replication. This complex also contributes to stalled replication forks' integrity and replication recombination intermediates' removal (see [7] for review), all cellular processes that can modulate the response to PARPi [8]. In parallel to this *in vitro* approach, the expression profiles of key PARP genes in a panel of control liver and HCC peritumor (PT) and tumor (T) tissues was determined. Indeed, PARP expression is a prerequisite for the use of PARPi and to investigate whether targeting PARP activity is an option for HCC therapy the transcript profiles of three PARP genes together with that of poly(ADP-ribose) glycohydrolase (PARG) that degrades the polymers and the protein levels of the major PARP protein PARP1 were also evaluated. In addition, as the cellular consequences of PARP inhibition can depend on cell proliferation rates [8] the transcript and protein expression profiles of the proliferation marker MKI67 were determined together with the protein levels of the surrogate DNA damage marker gammaH2AX (also known as serine 139 phosphorylated Histone H2AX) [9] in order to assess DNA damage levels during liver disease progression.

Materials and methods

Cell lines

The human hepatoma cell line HepG2 (ATCC HB-8065) and its derivatives HepG2 2.2.15 carrying the HBV wildtype genome and HepG2 K6 carrying a mutant form of HBV with no HBx protein [10, 11], Non-differentiated HepaRG cells expressing the tetracycline inducible promotor (HepaRG TR) or

the HBx protein under the tetracycline inducible promotor (HepaRG TRX) [11], HepaRG TRX sh-scramble expressing an in-efficient shRNA construct in a lentiviral GFP vector (Origene) and HepaRG TRX sh-SMC6 cells expressing a 29mer shRNA construct targeting the SMC6 transcript (Origene), Hep3B (ATCC HB-8064) and PLC/PRF/5 (ATCC CRL-8024) cells were grown in a humidified 37°C incubator under 5% CO_2.. All cell lines were regularly checked for mycoplasma contamination.

Cytotoxicity measurements

Cell survival was assessed using the colony formation assay for all cell models except the non-differentiated HepaRG TRX-based lines. Cells were seeded (1000 – 2000/25cm^2 flask) and left to adhere overnight before treatment. The PARPi Talazoparib (DMSO, 10uM) or Veliparib (PBS, 4mM) (Selleckchem, USA) were added directly to cell culture medium to achieve the final concentrations required. To assess the impact of PARP inhibition combined with IR, PARPi were present in the culture medium for 24h with the radiation delivered 1h after their addition. Cells were irradiated using a 6-MeV γ-ray clinical irradiator (SL 15 Phillips) at the Anti-Cancer Centre Léon-Bérard (Lyon, France) with a dose rate of 6Gy min^{-1} to give the required dose.

To assess hydroxurea's (HU) impact on cell survival, HU (Sigma, 0.2M in PBS) was added directly to culture medium (final concentration 2mM) for a period of 24h.

After drug removal and replacement of culture medium, colonies were grown under standard culture conditions for 10 days, then fixed in methanol and stained with 0.05% Coomassie brilliant blue in 3:1:6 ethanol/acetic acid/water. Colonies with more than 50 cells were counted and the surviving fraction (the colony count relative to mock-treated cells) determined.

Cell growth rates in non-differentiated HepaRG TRX-based lines were assessed by plating cells at a fixed density and allowing them to grow for the required time after treatment before counting viable cell numbers.

Western Blot

Cells (2.10^6) were lysed in RIPA buffer (50mM Tris pH7.4, 250mM NaCl, 0.1% SDS, 2mM DTT, 0.5% NP40) containing a protease inhibitor cocktail (Halt™) (30min, 4°C) or in 2% SDS in water containing Halt™ and sonicated for 10x 30s and centrifuged (15min, 4°C, 13,000g). Protein concentrations were estimated using the BCA Protein Assay (Pierce™). Samples were diluted in Laemmli 5X, boiled and 20µg protein extract loaded per lane. Proteins were separated on 8% (SMC6 detection) or 12% acrylamide gels and after transfer to nitrocellulose membranes were incubated with primary antibodies overnight at 4°C (1:1000 anti-gammaH2AX (Abgent ab18311), 1:1000 anti-H2AX (Cell Signalling 2595), 1:500 anti-Smc6 (Abgent AT3956a), 1:1000 pADPR (Abcam, clone ab14459)) except for anti-β-actin (1:10000 anti-β-actin (Sigma-Aldrich A1978) 1h, room temperature. Membranes were then incubated (1h, room temperature) with Horseradish-peroxidase-conjugated

secondary antibodies (1:10000). Detection used ECL (BioRad), ChemiDoc and Image Lab software (Bio-Rad).

Flow cytometry

To assess the impact of HU treatment on cell cycle progression HepG2, HepG2 2.2.15, HepG2 K6 and HepaRG TRX (non-differentiated, induced or not) ($2x10^6$ cells/$25cm^2$ flask) were seeded and left to attach overnight before treating with 2mM HU for varying times. Cells were then processed using the BD Cycletest™ Plus DNA reagent kit (Becton Dickinson) containing propidium iodide according to the manufacturer's protocol. Flow cytometric analysis was performed using a FACSCalibur cytofluorometer (Becton-Dickinson Biosciences). At least 10^4 events were recorded and data analysis was done with CellQuest Pro software (Becton-Dickinson Biosciences).

Immunofluorescence protein detection

The presence of gammaH2AX foci in irradiated cells was assessed by immunofluorescence. Cells were plated on coverslips (after induction in the case of the non-differentiated HepaRG TRX cells) and allowed to adhere overnight before irradiation as described above. Cells were returned to the incubator to allow DNA repair to proceed and then fixed (15min, room temperature, 4% formaldehyde), washed twice in PBS and permeabilized in ice cold lysis solution (0.5% Triton, 10.5% Sucrose, 0.06% $MgCl_2$, 20mM Hepes pH7, 50mM NaCl, 3min) before incubation (40min, 37°C) with anti-gammaH2AX (Abgent ab18311) (1:1000) in blocking buffer (PBS-BSA 3%) and incubation with an IgG secondary antibody (1:200), Alexa 488 (Fluor®) (20min, 37°C). After washing, coverslips were mounted with medium containing 4,6-diamidino-2-phenylindole (DAPI; Duolink®). Immunofluorescence images were acquired using an upright microscope Nikon NIE. At least 200 cells were analysed per experimental condition. The number of foci was quantified in arbitrary units (AU) by a macro using Image J software developed by J. Jacquemetton (CRCL, Lyon).

Expression shSMC6/Shcontrol for RNA seq analysis

Non-differentiated HepaRG TR, TRX, TRX+shscramble (control) and TRX+shSMC6 (construct C) cells ($1x10^6$) were seeded in 6-well plates and left to attach before tetracycline induction (1µg/ml) or not, for 4 days. SMC6 depletion was validated by western blot as previously described [6] and RNA extraction performed using RNeasy™ following manufacturer instructions. Three independent experiments were carried out.

RNA samples were sequenced using Illumina's NextSeq following standard procedures. Resulting base called sequences were demultiplexed with Bcl2fastq v2.17.1.14 using 0 mismatch, followed by trimming with cutadapt v1.9.1 and quality check with fastQC. Reads were mapped against hg19 genome (GRCH37, Feb. 2009) using TopHat v2.1.0 with default parameters (bowtie 2.2.9), and signals were normalized using cufflinks v2.1.1 which uses the FPKM (Fragments Per Kilobases of exon per Million mapped reads) method.

After preprocessing, FPKM values, corresponding isoform annotations, and phenotype data, were imported into R for further analysis with R/Bioconductor packages. Boxplots of normalized signals, hierarchical clustering, and multidimensional scaling were used for data inspection. Based on this, one outlier on each experimental group was removed at this step.

To define differentially expressed genes, we modelled experimental conditions as categorical variables in a linear regression using an empirical Bayesian approach [12] Pairwise comparisons with a False Discovery Rate (FDR)-adjusted P value below 0.05 and a fold-change of at least two, were considered statistically significant. Overlaps between gene sets were performed with the VennDiagram packages.

Patients and liver samples

180 HCC patients treated by surgical resection, included between 1996 and 2014 from three French clinical centres (Lyon Croix Rousse and Toulouse Hospitals and the French National Biological Resource Centres) were retrospectively studied (Agreement DC-2008-235). RNA samples were available from matched T and PT (at least 2 cm distant from the T) tissues for 150 patients and for the other 30 only T RNA samples were analysed. Protein extracts were available from 93 tissues (46 T, 47 PT) of the following aetiologies; 29 alcohol (13 T, 16 PT), 32 HBV (17 T, 15 PT) and 32 HCV (16 T,16 PT).

RNA samples from 11 and protein extracts from 8 surgically resected normal liver tissues surrounding colorectal adenocarcinoma metastasis (Centre Léon Bérard Biological Resource Centre, ministerial agreements #AC-2013-1871 and DC-2013-1870) were used as control samples respectively. Signed informed written consents in compliance with the requirements of the local ethical committee were obtained from patients before surgery.

RNA extraction and cDNA preparation

Total RNA was extracted from frozen tissues with Extract-all (Eurobio) according to the manufacturer's instructions. One µg was treated with DNAse-I (Roche) and then retro-transcribed (RT) using the SuperScript III First-Strand Synthesis System (Thermofischer), according to the manufacturer's instructions.

Quantitative real-time PCR

Primers for *GUS* used an endogenous control were designed using Oligo 5 (National Biosciences, Plymouth, MN, USA) and their specificity checked by searches in dbEST and nr databases. Primers for *PARP1*, *PARP2*, *PARP3*, *PARG* and *MKI67* and the PCR reaction conditions are described elsewhere [13]. Quantitative values for the different transcripts were obtained from the cell cycle number (Ct value) at which the fluorescent signal became exponential. Results, were expressed as target gene expression relative to the *GUS* gene.

Protein extraction and Reverse Phase Protein Array (RPPA) analysis

Protein extracts were prepared from frozen liver sections as previously described [14] and stored at -80° until further processing from 93 tissues from HCC patients (46 T, 47 PT) of the following aetiologies; 29 alcohol (13 T, 16 PT), 32 HBV (17 T, 15 PT) and 32 HCV (16T,16 PT). 8 surgically resected normal liver tissues served as controls.

Protein concentration was determined (Pierce BCA reducing agent compatible kit, ref 23252) and extracts printed onto nitrocellulose covered slides (Supernova, Grace Biolabs) using a dedicated arrayer (2470 arrayer, Aushon Biosystems) in five serial dilutions (1500 to 93.75 µg/ml) and three replicates per dilution. Arrays were labeled with 4 specific antibodies (H2AX 1:2000 (CST 2595); Phospho-Histone H2AX (ser139) 1:1000 (Abcam ab2893); PARP (uncleaved) 1:1000 (Abcam ab32378); Ki67 1:250 (DAKO M7240) as described in [15]. Read-out was done using IRDye 800CW (LiCOR) on an Innoscan 710-AL scanner (Innopsys). For staining of total protein, arrays were incubated 30 min in Super G blocking buffer (Grace Biolabs), rinsed in water, incubated 5min in 0.000005% Fast green FCF (Sigma) and rinsed again in water. Raw data were normalized using Normacurve [16].

Statistics

The distributions of the gene mRNA levels were characterised by their median values and ranges using GraphPad Prism software (version 7.05.237). For the unsupervised hierarchical clustering of the RPPA data, Pearson was used as a distance measure and Ward as the clustering algorithm. Paired *t*-tests, Mann Whitney test, Kruskal Wallis test, Fisher's exact, Wilcoxon matched-pairs signed rank test and Spearman rank correlation test were used as appropriate. Differences were considered significant at confidence levels greater than 95% ($P \leq 0.05$)

Other materials and methods

Additional information regarding cell culture conditions, inducible lentiviral vectors and online data for HCC livers, are provided as Supplementary Materials and Methods.

Results

In vitro assessment of sensitivity to the PARP inhibition alone and in combination with IR

Our previous *in vitro* studies showed variability in PARPi sensitivity with a short (2h) exposure to Veliparib (10µM) reducing clonogenic survival in HepG2 but not PLC/PRF/5 or Hep3B liver cells [5]. However, in both HepG2 and the more radiation resistant PLC/PRF/5 cells, PARP inhibition lowered IR-induced cell survival based on the mean lethal dose (D_{37})[5]. We demonstrate here that a longer Veliparib (10µM) exposure (24h) significantly decreased cell survival in all three cell models (Figure 1). In addition, exposure to a second PARPi, Talazoparib, chosen because it is a more potent PARPi than Veliparib in terms of induced cytotoxicity [17] at a dose (50nM/24h) that inhibited PARP activity as assessed by polyADPribose levels after doxorubicin treatment (Supplementary Figure 1B), significantly lowered cell survival compared to untreated cells. Under these experimental conditions a

differential impact between the two PARPi on cell survival was only seen in HepG2 cells (54.2 ± 12.7% Veliparib vs 33 ± 7.9% Talazoparib, $P \leq 0.001$) (Figure 1A).

When combined with a fixed 2Gy X-ray dose Veliparib (10μM/24h) exposure significantly attenuated the radiation sensitivity of HepG2 (Figure 1A) and Hep3B (Figure 1C) but not PLC/PRF/5 cells (Figure 1B). In contrast, the combined treatment of Talazoparib (50nM/24h) and X-rays (2Gy) significantly lowered cell survival in all three models compared to radiation treatment alone, with the lowest survival seen in HepG2 cells (9.5 ± 4.2%) (Figure 1A). As Hep3B cells are reported to be both HR and NHEJ repair competent (see for instance [18]), the impact of 10-fold higher inhibitor doses was also investigated. These higher inhibitor doses significantly reduced cell survival with Talazoparib alone and in combination with radiation having a significantly greater impact than either Veliparib +/- radiation exposure (Figure 1C).

Impact of HBx viral protein on cell survival after IR and PARP inhibition

As HBx expression leads to the degradation of the cell's SMC5/6 complex that is involved in processes that could modulate the impact of PARPi we next examined its impact on cell survival using HepG2-derived cell lines differing in HBx expression: HepG2 2.2.15 cells express the whole HBV genome [10] and HepG2 K6 cells carry a mutant HBV that encodes all HBV proteins except HBx [11]. In the absence of an efficient antibody against HBx, its expression was routinely deduced from SMC6 degradation in cellular protein extracts using western blotting (Supplementary Figure 1Ai).

Under the experimental conditions tested, the clonogenic survival after treatment with either Veliparib (10μM/24h) +/- X-rays (2Gy) was significantly lower in the presence of HBx (Figure 2A). A second non-tumoral cell model (HepaRG TRX) was also investigated in which HBx is transiently induced for 5 days thus reducing longer-term selection effects or adaption to HBx expression. In the HepaRG TRX model HBx expression had no effect on relative cell numbers after Veliparib exposure (24h/10μM) but cell growth was significantly reduced after Talazoparib (24h/50nM) (Figure 2B) or IR (4Gy X-rays) exposure. The combination of Talazoparib and IR significantly attenuated relative cell growth compared to radiation exposure alone. These response profiles probably reflect both the higher efficiency of PARP1 trapping by Talazoparib and the involvement of the SMC5/6 complex in the removal of such complexes in replicating cells.

DNA damage levels were next assessed in the HBx-expressing cells after X-ray exposure (4Gy) using the formation and persistence of gamma-H2AX foci as a surrogate DNA DSB marker. A rapid increase in gammaH2AX foci/cell was seen after radiation exposure with a subsequent decline in foci numbers in the HepG2 parental and HepG2 K6 cells starting 30min/1h post-irradiation. In contrast, in HepG2 2.2.15 foci levels remained at the high levels seen initially after treatment over the first 2h post-irradiation after which a decline in numbers was noted. However, foci numbers remained substantially higher than in HepG2 and HepG2 K6 cells at later time points studied suggestive of

altered DNA repair capacity (Figure 2C). Similarly, in the HepaRG model a delayed repair of DNA damage was observed in the HBx-expressing cells with higher numbers of foci persisting until 4h post-irradiation after which a decline in numbers was observed (Figure 2D) in support of the persistence of higher levels of DNA damage in the presence of HBx and associated with SMC5/6 complex loss.

HBx viral protein affects survival under replicative stress

As the SMC5/6 complex is also involved in a late step of cellular DNA replication, the sensitivity of HBx-expressing cells to HU induced cell killing was next assessed. This potent inhibitor of ribonucleotide reductase depletes the cellular dNTP pool resulting in stalled replication forks that, after a prolonged HU treatment (24h/2mM), collapse into DSBs resulting in S-phase cell cycle checkpoint activation. Under these exposure conditions HBx-expressing HepG2 2.2.15 cells had a significantly lower survival than either the parental or HepG2 K6 cells (Figure 3Ai). A significant reduction in relative cell growth was also seen in HBx-expressing HepaRG cells (Figure 3Bi).

The presence of blocked replication forks and the generation of DSBs caused by HU treatment will activate the intra-S cell cycle checkpoint to block the exit from S-phase of cells allowing time for DNA repair to occur. Whilst no HBx-dependent difference in the proportion of cells in S-phase were seen after HU treatment in either cell model (Figure 3Aii/Bii), HBx-expressing cells had higher levels of gammaH2AX 24h after HU treatment indicative of higher persisting levels of DNA DSBs (Figure 3Aiii/Biii). These profiles would suggest that the sensitivity to the cell killing effects of HU associated with HBx expression was due to an impairment in the processing of DNA strand breaks and not a defect in cell cycle checkpoint activation.

Is the HBx-associated cell sensitivity due to the degradation of SMC6 or other transcriptional changes?

As a first approach to address whether the sensitivity to IR, HU and PARPi in HBx-expressing cells is solely due to SMC5/6 complex degradation or whether HBx modulates other DNA Damage response (DDR) components that in-turn impacts on sensitivity to these agents we compared the transcriptome of proliferating HepaRG tetracycline-induced HBx cells *vs* cells depleted in SMC6 using an sh-targeting approach. Most differentially expressed genes were unique to each of these two conditions with only 24 total overlapping genes (Supplementary Figure 2). Of note no significant changes in the transcript levels of the PARP transcripts (PARP1, PARP2 and PARP3) or PARG were noted when either HBx was induced or SMC6 depleted.

Next, we focused on those genes commonly up- or down-regulated by HBx induction and SMC6 depletion, with the assumption that these genes are surrogate markers of SMC6 loss under HBx expression. Ten genes displayed such behaviour (Table 1 and Supplementary Table 1). Three were significantly down-regulated (PARPBP (also known as PARI), PBLD and LRRCC1) of which PARPBP has a potential DDR role and thus could contribute to the increased sensitivity seen in HBx-

expressing cells to the panel of DNA damaging agents tested. Seven genes showed an up-regulation (SRPK2, YAF2, PRR19, HSPB3, CA12, SP3 and SRPRA).

In addition to these overlapping genes, 27 genes were down- and 33 up-regulated when HBx was expressed and 89 genes were down- and 31 up-regulated when SMC6 was depleted (Supplementary Figure 2, Supplementary Tables 2 and 3). KCNV1 and ZNF showed alternative splicing when HBx was expressed. DDR genes did not appear to be over-represented in these panels. For instance, no changes in BRCA1 or RAD51 transcript levels that can influence PARP inhibitor sensitivity [17] were noted. However, BABAM2 and RAD52 expression, both encoding genes involved in DSB repair, were increased in the presence of HBx. This might be a compensation mechanism for the loss of SMC6 and clearly needs further investigation.

Profile of PARP gene expression and DNA damage levels in HCC tissues

To determine the expression profile of PARP genes in HCC tissues, we assessed PARP1, PARP2 and PARP3 transcript levels together with those of PARG and MKI67 in PT and matched T tissues from a cohort of individuals with HCV-, HBV-, NASH- and alcohol-associated HCCs with or without cirrhosis (cohort characteristics are detailed in Supplementary Table 4) compared to a panel of control liver tissues. A significant increase in all the transcript studied was observed in T compared to PT tissues (Figure 4A). Cirrhosis in PT tissues was associated with significantly higher transcript levels of PARG, PARP2, PARP3 and MKI67 compared to non-cirrhotic PT tissues but only for PARP2 were levels significantly higher than control tissues (Figure 4B). Significantly higher levels of all the transcripts were found in T tissues compared to PT or control tissues irrespective of cirrhosis status.

In terms of aetiology-specific transcript profiles, only PT tissues from HCV-associated HCCs had significantly higher levels of PARP2 and MKI67. This difference may in part reflect that HCV-associated PT tissues had the highest proportion of tissues with cirrhosis. For all 4 aetiologies PARP1, PARP2 and MKI67 transcript levels were significantly higher in T than corresponding PT tissues, with increases in PARG seen in T compared to PT tissues from HCV-, HBV- and alcohol-associated HCCs and for PARP3 in HBV- and alcohol-associated HCCs (Figure 4C).

Protein extracts available from a subset of HCV, HBV and alcohol-associated HCC tissues were used to assess the protein expression levels of PARP1, MKI67, gammaH2AX and H2AX. RPPA validated antibodies were not available for the other genes investigated. First, we assessed if PARP1 or MKI67 mRNA and protein levels were correlated. Weak but significant correlations for PARP1 ($r=0.31$, $P=0.0387$), and MKI67 ($r=0.45$, $P=0.0005$) mRNA/protein levels (Supplementary Figure 3A) were found in T tissues but not in control or PT tissues (data not presented). Next, we assessed the variation in protein levels during disease progression. A non-supervised hierarchical clustering of the results (Supplementary Figure 3B) suggests the presence of at least two major subgroups of samples, cluster A being enriched in T samples, while cluster B contains more PT and controls (Chi-square test $P=0.0003$), suggesting that T and PT samples differ in their expression levels for the measured

proteins. Yet, despite higher transcript levels in T tissues compared to control and PT tissues, no significant increases in protein levels were found for PARP1 and MKI67 (P=0.382, P=0.078 respectively) (Figure 5A). However, lower H2AX levels were associated with disease progression from control to PT to T tissues, whereas gammaH2AX levels increased, resulting in a significant increase in the ratio of gamma-H2AX/H2AX (Figure 5B). Gamma-H2AX is an integrated marker of DNA damage and repair levels and an extremely sensitive organismal stress indicator [9]. Increasing gamma-H2AX levels during HCC tumorigenesis are thus indicative of increased stress and DNA damage and might contribute to the vulnerability to PARP inhibition.

Discussion

This study has shown that *in vitro* HCC models are sensitive to the cell killing effects of PARPi when used as a single agent and that PARPi significantly attenuated radiation sensitivity in all the liver models tested. Our data is also in agreement with the literature that Talazoparib is a more potent PARPi than Veliparib in terms of induced cytotoxicity [17]. Whilst the cytotoxic activities of PARPi were initially related to their ability to block DNA single strand break repair, it is now recognized that additional cytotoxic mechanisms exist including the generation of PARP-DNA complexes which block replication [17]. Indeed, stalled replication forks are a major source of genome instability in proliferating cells and strategies that exacerbate replication stress are a promising avenue to improve anticancer therapies (see [19]). The presence of the HBx protein increased this cytotoxicity which can in part be explained by the increased replicative stress concomitant to the HBx-induced loss of the SMC5/6 complex. Of the genes modulated in HBx-induced and SMC5/6 depleted cells, whilst no changes in the PARP transcripts studied were noted, the reduction in PARPBP transcript levels may contribute to these increases. Indeed, PARPBP depletion has been shown to enhance replication stress and DNA-damage accumulation [20] which is concordant with the *in vitro* cellular phenotype of the HBx-expressing cells. It has been recently reported that, based on The Cancer Genome Atlas (TCGA) and Human Protein Atlas databases, PARPBP was significantly upregulated in HCC tissues compared with normal liver tissues ($P \leq 0.05$) and correlated with worse overall survival and recurrence-free survival [21]. Of the other genes down-regulated in HBx-expressing/SMC6 depleted cells PBLD was reported down-regulated in HCC tissues [22]·[23], suggesting that it's expression can be modulated by HBx-independent mechanisms, with this deletion found to be an independent poor prognosis predictor in HCC patients [23].

In addition to transcriptional modulation, it cannot be excluded that the effect of HBx on *in vitro* cell survival and DNA damage levels may be related to protein/protein interactions with a partner implicated in DDR pathways as seen for the HBx-induced loss of the SMC5/6 complex. Whilst a comprehensive proteomics evaluation of the impact of HBx expression was outside the scope of this present study, altered DDR protein expression have been reported in HBx-expressing models that

potentially could impact on cell survival. For instance, in HBx-transgenic mice decreased expression of Mre11 and Rad51 expression has been noted [24]. HBx can also bind the tumour suppressor protein p53 that can modulate both DNA strand break repair pathways [25] and nucleotide excision repair [26].

Gene expression analysis carries the potential to dissect the molecular heterogeneity of cancers and can distinguish on this basis sub-classes for certain cancer types, including HCC [27]. Unfortunately, this increasing knowledge has not yet resulted in biomarker discovery. Thus, improved clinical care and identifying the most relevant characteristics of HCC and personalised medicine remains a major challenge. A comprehensive review of the expression profiles of 450 human DDR genes in different cancers [28] highlighted the therapeutic opportunities for targeting DDR, however, for HCC data was only available for 18 T samples. Subsequent bioinformatics analyses of a panel of 59 DNA repair genes in the HCC data from the TCGA to define a co-regulated gene cluster would suggest that DNA repair stratification could be useful for predicting prognosis and designing clinical trials for targeted therapy [29]. A recent analysis of the response to 31 anticancer agents in a large panel of liver cancer cell lines whose protein, RNA and mutational signatures resembled that of the aggressive proliferation class of HCC, identified genetic alterations and gene expression patterns associated with response to these agents [30]. This information might be used to select patients for clinical trials but did not extend to DNA repair inhibitors such as PARPi that are proving promising for other cancer types. In addition, based on the impact of HBx observed here it would be of interest to determines its expression profile in HBV-associated PT and T tissues to determine whether it can impact on therapeutic responses.

There is some limited information on PARP family gene and protein expression profiles in HCC. In agreement with our data, increased PARP1 mRNA expression was reported based on the online TCGA HCC dataset [31] (and Supplementary Figure 4) and in Chinese populations [31, 32] but not found in a Polish population [33]. In our study, no correlation was found between mRNA and protein levels and no increase in PARP1 protein levels was observed in T tissues relative to control and PT tissues. This is in contrast to the data of Li *et al* [31] and Xu *et al* [34] who reported higher PARP1 protein levels in HCC T tissues. In agreement with our data PARP2 and PARG mRNA expression was elevated in T samples compared to the matched non-T samples in the on-line TCGA HCC dataset, however, no increases were seen for PARP3. The reasons for these discrepancies remain to be established but may be due to technical issues relating to antibody choice and tissues used for comparative purposes and reflect differences in the compositions of tissue panels and the impact of etiology on expression profiles. The elevated gammaH2AX seen in both this study and Evert *et al* [35] are indicative of a higher DNA damage burden and/or replication stress that could be interpreted as an imbalance in DSB repair in HCC tissues and has been associated with cancer progression in many cancer types (see for example [36]). Intriguingly this increase is accompanied here by a

reduction in H2AX levels during progression from control to T tissue. These changes parallel observations by Grusso and colleagues in triple negative breast cancer patients where chronic oxidative stress promotes H2AX degradation [37]. HCC is considered an inflammation-associated cancer, thus it is tempting to speculate that oxidative stress may be the underlying cause of the reduction in H2AX levels associated with liver disease progression. Grusso and colleagues also noted that a ROS-mediated H2AX decrease was observed after chemotherapy and was an indicator of the therapeutic efficiency and survival in Triple Negative Breast Cancer patients [37]. Whether combining PARP inhibitors that would block repair, with radiotherapy that would not only generate oxidative stress and thus further reduce H2AX levels, but also cytotoxic DNA damage, would enhance HCC tumour cytotoxicity and thus be beneficial in a therapeutic setting or lead to increased genomic instability and its consequences would need to be investigated in clinical trials.

Conclusion

In conclusion, the *in vitro* potentiation of cell death by PARPi alone or in combination with radiation exposure, taken together with the observations of elevated DNA damage levels in HCC T tissues, may represent a vulnerability that can be exploited for therapeutic benefit. Indeed, whilst RT has not been widely used for HCC treatment, it is a choice that needs further clinical evaluation [2] [3]. In addition to their direct impact on the DDR response, PARPi may have additional therapeutic benefits. For instance, the combination of IR and PARP inhibition can improve the vasculature leading to the reoxygenation of hypoxic T tissues, thus bypassing hypoxia-induced radioresistance (see [5] and references therein). Additionally, PARP inhibition can trigger the STING-dependent immune response and enhance the therapeutic efficacy of immune checkpoint blockade independent of BRCAness [38]. As the synergy between RT and the immune response is well documented the question arises if combining PARP inhibition, radiation, and immunotherapy could be a possible treatment strategy (see review [39]) and in particular for HCC where there is a growing body of evidence for each individually as therapeutic options.

Acknowledgments

The authors would like to thank Hien Luong Nguyen, Magali Jacquet, Loïc Peyrot and Lydie Lefrancois who contributed to early stages of this project, David Cox, Agnes Tissier and Virginie Petrilli (CRCL, Lyon) for helpful discussions, J. Jacquemetton (CRCL, Lyon) for the development of macros for counting foci and Adeline Granzotto (CRCL, Lyon) for organising the irradiation of cells. The authors thank Pr. M. Rivoire (Centre Léon Bérard, Lyon) for providing human liver tissues.

References

[1] Calderaro J, Couchy G, Imbeaud S, Amaddeo G, Letouzé E, Blanc J-F, et al. Histological subtypes of hepatocellular carcinoma are related to gene mutations and molecular tumour classification. Journal of Hepatology 2017;67(4):727-38.

[2] Ohri N, Dawson LA, Krishnan S, Seong J, Cheng JC, Sarin SK, et al. Radiotherapy for Hepatocellular Carcinoma: New Indications and Directions for Future Study. JNCI: Journal of the National Cancer Institute 2016;108(9): djw133.

[3] Chino F, Stephens SJ, Choi SS, Marin D, Kim CY, Morse MA, et al. The role of external beam radiotherapy in the treatment of hepatocellular cancer. Cancer 2018;124(17):3476-89.

[4] Guillot C, Hall J, Herceg Z, Merle P, Chemin I. Update on hepatocellular carcinoma breakthroughs: Poly(ADP-ribose) polymerase inhibitors as a promising therapeutic strategy. Clinics and Research in Hepatology and Gastroenterology 2014;38(2):137-42.

[5] Guillot C, Favaudon V, Herceg Z, Sagne C, Sauvaigo S, Merle P, et al. PARP inhibition and the radiosensitizing effects of the PARP inhibitor ABT-888 in in vitrohepatocellular carcinoma models. BMC Cancer 2014;14(1):603.

[6] Decorsière A, Mueller H, van Breugel PC, Abdul F, Gerossier L, Beran RK, et al. Hepatitis B virus X protein identifies the Smc5/6 complex as a host restriction factor. Nature 2016;531:386-9.

[7] Aragón L. The Smc5/6 Complex: New and Old Functions of the Enigmatic Long-Distance Relative. Annual Review of Genetics 2018;52(1):89-107.

[8] Mégnin-Chanet F, Bollet MA, Hall J. Targeting poly(ADP-ribose) polymerase activity for cancer therapy. Cellular and Molecular Life Sciences 2010;67(21):3649-62.

[9] Bonner WM, Redon CE, Dickey JS, Nakamura AJ, Sedelnikova OA, Solier S, et al. γH2AX and cancer. Nature Reviews Cancer 2008;8(12):957-67.

[10] Sells MA, Zelent AZ, Shvartsman M, Acs G. Replicative intermediates of hepatitis B virus in HepG2 cells that produce infectious virions. Journal of Virology 1988;62(8):2836-44.

[11] Lucifora J, Arzberger S, Durantel D, Belloni L, Strubin M, Levrero M, et al. Hepatitis B virus X protein is essential to initiate and maintain virus replication after infection. Journal of Hepatology 2011;55(5):996-1003.

[12] Smyth Gordon K. Linear Models and Empirical Bayes Methods for Assessing Differential Expression in Microarray Experiments. *Statistical Applications in Genetics and Molecular Biology.* 3. 2004:1.

[13] Bieche I, Pennaneach V, Driouch K, Vacher S, Zaremba T, Susini A, et al. Variations in the mRNA expression of poly(ADP-ribose) polymerases, poly(ADP-ribose) glycohydrolase and ADP-ribosylhydrolase 3 in breast tumors and impact on clinical outcome. International Journal of Cancer 2013;133(12):2791-800.

[14] Bonnin M, Fares N, Testoni B, Estornes Y, Weber K, Vanbervliet B, et al. Toll-like receptor 3 downregulation is an escape mechanism from apoptosis during hepatocarcinogenesis. Journal of Hepatology 2019;71(4):763-72.

[15] Meseure D, Vacher S, Lallemand F, Alsibai KD, Hatem R, Chemlali W, et al. Prognostic value of a newly identified MALAT1 alternatively spliced transcript in breast cancer. British Journal of Cancer 2016;114(12):1395-404.

[16] Troncale S, Barbet A, Coulibaly L, Henry E, He B, Barillot E, et al. NormaCurve: A SuperCurve-Based Method That Simultaneously Quantifies and Normalizes Reverse Phase Protein Array Data. PLOS ONE 2012;7(6):e38686.

[17] Murai J, Huang S-Y, Das BB, Renaud A, Zhang Y, Doroshow JH, et al. Trapping of PARP1 and PARP2 by Clinical PARP Inhibitors. Cancer Research 2012;72(21):5588-99.

[18] Zhang L, Zhang F, Zhang W, Chen L, Gao N, Men Y, et al. Harmine suppresses homologous recombination repair and inhibits proliferation of hepatoma cells. Cancer Biology & Therapy 2015;16(11):1585-92.

[19] Liao H, Ji F, Helleday T, Ying S. Mechanisms for stalled replication fork stabilization: new targets for synthetic lethality strategies in cancer treatments. EMBO reports 2018;19(9):e46263.
[20] Nicolae CM, O'Connor MJ, Schleicher EM, Song C, Gowda R, Robertson G, et al. PARI (PARPBP) suppresses replication stress-induced myeloid differentiation in leukemia cells. Oncogene 2019;38(27):5530-40.
[21] Yu B, Ding Y, Liao X, Wang C, Wang B, Chen X. Overexpression of PARPBP Correlates with Tumor Progression and Poor Prognosis in Hepatocellular Carcinoma. Digestive Diseases and Sciences 2019;64(10):2878-92.
[22] Long J, Lang Z, Wang H, Wang T, Wang B, Liu S. Glutamine synthetase as an early marker for hepatocellular carcinoma based on proteomic analysis of resected small hepatocellular carcinomas. Hepatobiliary Pancreat Dis Int 2010;9(3):296-305.
[23] Li A, Yan Q, Zhao X, Zhong J, Yang H, Feng Z, et al. Decreased expression of PBLD correlates with poor prognosis and functions as a tumor suppressor in human hepatocellular carcinoma. Oncotarget 2015;7(1):524-37.
[24] Ahodantin J, Bou-Nader M, Cordier C, Mégret J, Soussan P, Desdouets C, et al. Hepatitis B virus X protein promotes DNA damage propagation through disruption of liver polyploidization and enhances hepatocellular carcinoma initiation. Oncogene 2019;38:2645-57.
[25] Menon V, Povirk L. Involvement of p53 in the repair of DNA double strand breaks: multifaceted Roles of p53 in homologous recombination repair (HRR) and non-homologous end joining (NHEJ). Subell Biohem 2014;85:321-36.
[26] Becker SA, Lee TH, Butel JS, Slagle BL. Hepatitis B virus X protein interferes with cellular DNA repair. J Virol 1998;72(1):266-72.
[27] Calderaro J, Ziol M, Paradis V, Zucman-Rossi J. Molecular and histological correlations in liver cancer. Journal of Hepatology 2019;71(3):616-30.
[28] Pearl LH, Schierz AC, Ward SE, Al-Lazikani B, Pearl FMG. Therapeutic opportunities within the DNA damage response. Nature Reviews Cancer 2015;15:166-80.
[29] Lin Z, Xu S-H, Wang H-Q, Cai Y-J, Ying L, Song M, et al. Prognostic value of DNA repair based stratification of hepatocellular carcinoma. Scientific Reports 2016;6(1):25999.
[30] Caruso S, Calatayud A-L, Pilet J, La Bella T, Rekik S, Imbeaud S, et al. Analysis of Liver Cancer Cell Lines Identifies Agents With Likely Efficacy Against Hepatocellular Carcinoma and Markers of Response. Gastroenterology 2019;157(3):760-76.
[31] Li J, Dou D, Li P, Luo W, Lv W, Zhang C, et al. PARP-1 serves as a novel molecular marker for hepatocellular carcinoma in a Southern Chinese Zhuang population. Tumor Biology 2017;39(7).
[32] Qi H, Lu Y, Lv J, Wu H, Lu J, Zhang C, et al. The long noncoding RNA lncPARP1 contributes to progression of hepatocellular carcinoma through up-regulation of PARP1. Bioscience Reports 2018;38(3).
[33] Krupa R, Czarny P, Wigner P, Wozny J, Jablkowski M, Kordek R, et al. The Relationship Between Single-Nucleotide Polymorphisms, the Expression of DNA Damage Response Genes, and Hepatocellular Carcinoma in a Polish Population. DNA and Cell Biology 2017;36(8):693-708.
[34] Xu X, Liu Z, Wang J, Xie H, Li J, Cao J, et al. Global proteomic profiling in multistep hepatocarcinogenesis and identification of PARP1 as a novel molecular marker in hepatocellular carcinoma. Oncotarget 2016;7(12):13730-41.
[35] Evert M, Frau M, Tomasi ML, Latte G, Simile MM, Seddaiu MA, et al. Deregulation of DNA-dependent protein kinase catalytic subunit contributes to human hepatocarcinogenesis development and has a putative prognostic value. British Journal Of Cancer 2013;109:2654-64.
[36] Bartkova J, Hořejší Z, Koed K, Krämer A, Tort F, Zieger K, et al. DNA damage response as a candidate anti-cancer barrier in early human tumorigenesis. Nature 2005;434(7035):864-70.

[37] Gruosso T, Mieulet V, Cardon M, Bourachot B, Kieffer Y, Devun F, et al. Chronic oxidative stress promotes H2AX protein degradation and enhances chemosensitivity in breast cancer patients. EMBO Mol Med 2016;8(5):527-49.
[38] Shen J, Zhao W, Ju Z, Wang L, Peng Y, Labrie M, et al. PARPi Triggers the STING-Dependent Immune Response and Enhances the Therapeutic Efficacy of Immune Checkpoint Blockade Independent of BRCAness. Cancer Research 2019;79(2):311-9.
[39] Césaire M, Thariat J, Candéias MS, Stefan D, Saintigny Y, Chevalier F. Combining PARP Inhibition, Radiation, and Immunotherapy: A Possible Strategy to Improve the Treatment of Cancer? International Journal of Molecular Sciences 2018;19(12):3793.

Table 1: Genes co-regulated by HBx expression and SMC6 loss[†]

Gene	Transcript	logFC Hbx[‡]	adj.P.Value[§]	logFC shSMC6[‡]	adj.P.Value[§]
PBLD	uc001jns.1	-10.03	9.15E-03	-8.78	1.59E-02
PARPBP	uc001tjk.3	-8.23	4.19E-04	-8.86	3.14E-04
LRRCC1	uc010lzz.2	-2.76	4.79E-02	-8.50	1.35E-04
HSPB3	uc003jph.2	5.84	5.89E-03	6.58	3.33E-03
SRPRA	uc010sbm.2	6.02	4.32E-02	8.75	5.80E-03
SP3	uc002uig.3	6.31	3.35E-02	8.09	8.33E-03
CA12	uc002ame.3	6.99	8.15E-03	7.59	5.37E-03
YAF2	uc010sko.2	7.89	7.68E-05	7.69	1.08E-04
PRR19	uc002oth.1	8.05	7.43E-04	6.83	1.92E-03
SRPK2	uc003vct.4	8.49	2.71E-05	10.10	2.62E-05

[†]Genes that are co-regulated by HBX expression and SMC6 loss are shown in bold in the Venn diagram (Supplementary Figure 2). [‡] log fold change in transcript expression in presence of HBx or loss of SMC6 (shSMC6), - represents a reduction in expression. [§] P values are false discovery rate corrected.

Fig.1. Clonogenic cell survival after PARP inhibition and/or IR exposure. Cell survival assessed by colony formation in (A) HepG2, (B) PLC/PRF/5 and (C) Hep3B cells after exposure to the PARP inhibitors Veliparib or Talazoparib (24h) and/or IR. (2Gy). Data represents the mean +/- SD of ≥ 3 independent experiments carried out in triplicate. *P ≤ 0.05, **P ≤ 0.01, ***P ≤ 0.001, ****P ≤ 0.0001, ns = non-significant. (Mann Witney U-test).

Fig. 2. Impact of HBx expression on cell survival and DNA damage levels. (A) Mean +/- SD survival in HepG2 2.2.15 (expressing HBx) or HepG2 K6 (no HBx) after Veliparib (24h) +/- IR (2Gy). (B) Mean +/- SD cell survival of HepaRG-TRX cells expressing HBx (+ tetracycline) or not after Veliparib or Talazoparib +/- IR. *P ≤ 0.05, **P ≤ 0.01, ***P ≤ 0.001, ****P ≤ 0.0001, ns = non-significant (Mann Witney U-test, data from ≥ 3 independent experiments). (C) GammaH2AX foci numbers after IR (4Gy) in HepG2-derived cells (one representative experiment, ≥ 200 cells/condition). (D) Mean +/-SD GammaH2AX foci numbers in HepaRG-TRX cells +/- HBx after IR (4Gy) (3 independent experiments, ≥ 200 cells/condition).

Fig. 3. Impact of HU on cell survival and cell cycle progression in HepG2 and HepaRG TRX-derived cells. (Ai and Bi) cell survival (mean +/- SD, ≥ 3 independent experiments) after HU (2mM/24h) exposure. (Aii and Bii) % of cells in the S phase of the cell cycle 24h after treatment with HU (2mM) (mean +/- SD, ≥ 3 independent experiments). (Aiii and Biii) Level of gammaH2AX in cell protein extracts after exposure to HU (2mM/24h). One representative experiment shown. **P ≤ 0.01, ***P ≤ 0.001, ****P ≤ 0.0001, ns = non-significant (Mann–Whitney U-test.)

Fig. 4. Variation in gene expression in Control and HCC tissues. (A) Comparison of normalised transcript levels in 11 control (CON) liver tissues, 148 PT and 140 T tissues. (B) Comparison of normalised transcript levels in 11 control (CON) liver tissues and PT tissues (93 cirrhotic, 55 non-cirrhotic) and T tissues (88 cirrhotic, 52 non-cirrhotic). (C) Comparison of normalised transcript levels between 11 CON liver tissues and HCV-associated (47 PT, 56 T), HBV-associated HCC (39 PT, 41 T), OH-associated HCC (42 PT, 54 T), and NASH-associated HCC (23 PT, 29 T) tissues. Error bars represent median and interquartile range *P ≤ 0.05, **P ≤ 0.01, ***P ≤ 0.001, ****P ≤ 0.0001, ns = non-significant (Mann-Whitney U-test for (A), Kruskal Wallis test for (B)).

Fig. 5. Comparisons of protein levels in control, PT and T HCC tissues. (A) Comparison of normalised PARP1 and Ki67 protein levels and (B) normalised H2AX and gammaH2AX protein levels and their ratio in comparison in control (CON) (8), PT (47) and T tissues (46) from HCV, HBV and NASH-associated tumors. *P ≤ 0.05, **P ≤ 0.01, ***P ≤ 0.001, ****P ≤ 0.0001, ns = non-significant (Kruskal Wallis test).

Figure 1

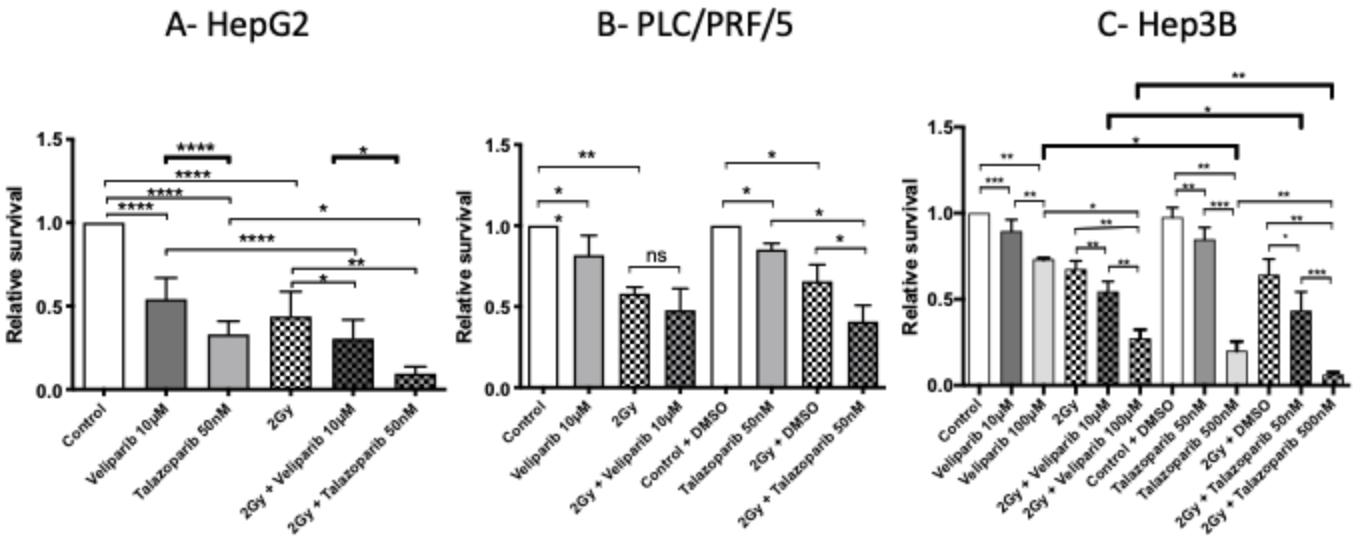
A- HepG2
B- PLC/PRF/5
C- Hep3B
Relative survival
1.5
1.0
0.5
0.0
Control
Veliparib 10µM
Talazoparib 50nM
2Gy
2Gy + Veliparib 10µM
2Gy + Talazoparib 50nM
ns
Control + DMSO
2Gy + DMSO
Veliparib 100µM
2Gy + Veliparib 100µM
Talazoparib 500nM
2Gy + Talazoparib 500nM

Figure 2

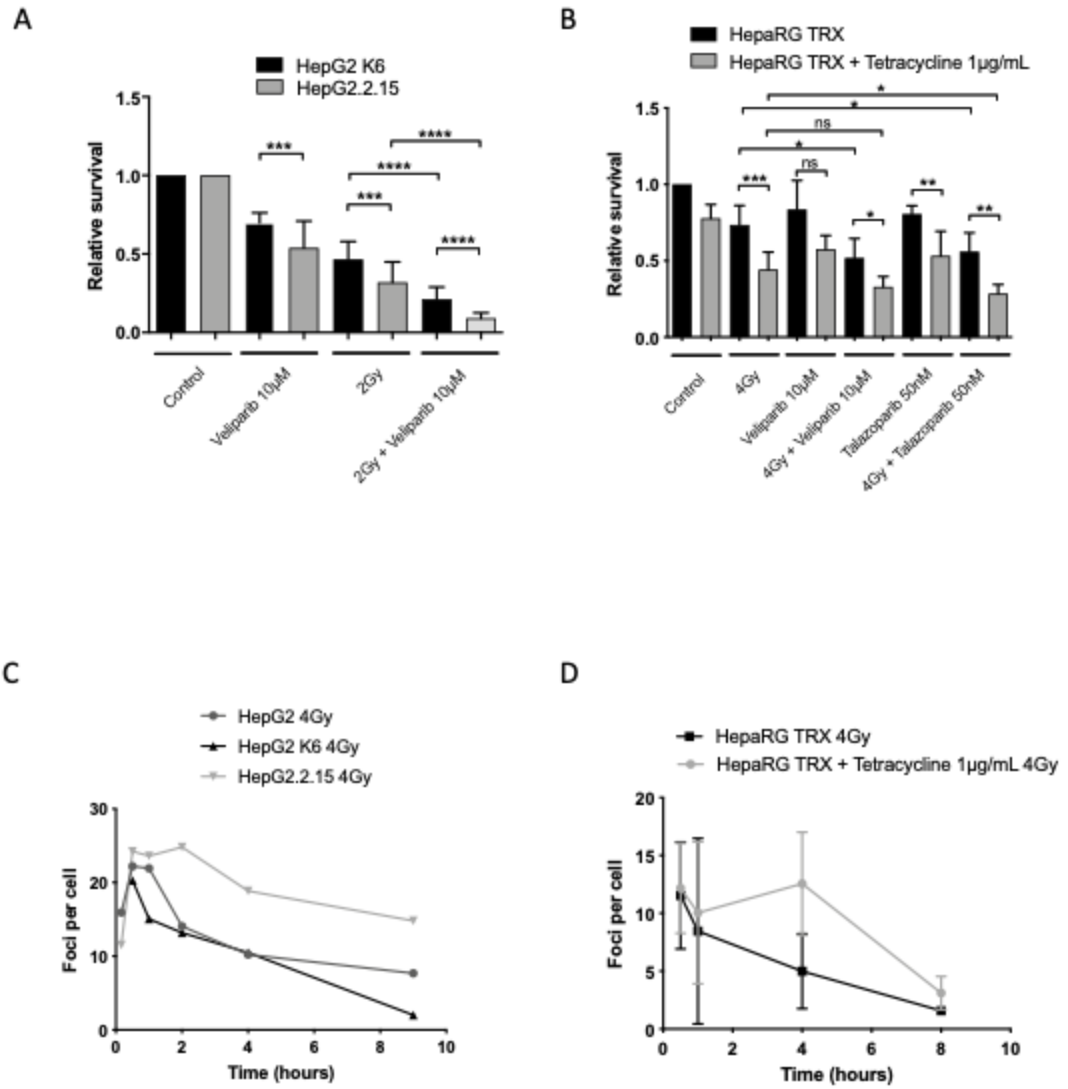
A
HepG2 K6
HepG2.2.15
Relative survival
1.5
1.0
0.5
0.0
***
****
***
****
****
Control
Veliparib 10μM
2Gy
2Gy + Veliparib 10μM
B
HepaRG TRX
HepaRG TRX + Tetracycline 1μg/mL
Relative survival
1.5
1.0
0.5
0.0
*
*
ns
*
ns
***
*
**
**
Control
4Gy
Veliparib 10μM
4Gy + Veliparib 10μM
Talazoparib 50nM
4Gy + Talazoparib 50nM
C
HepG2 4Gy
HepG2 K6 4Gy
HepG2.2.15 4Gy
Foci per cell
30
20
10
0
0
2
4
6
8
10
Time (hours)
D
HepaRG TRX 4Gy
HepaRG TRX + Tetracycline 1μg/mL 4Gy
Foci per cell
20
15
10
5
0
0
2
4
6
8
10
Time (hours)

Figure 3

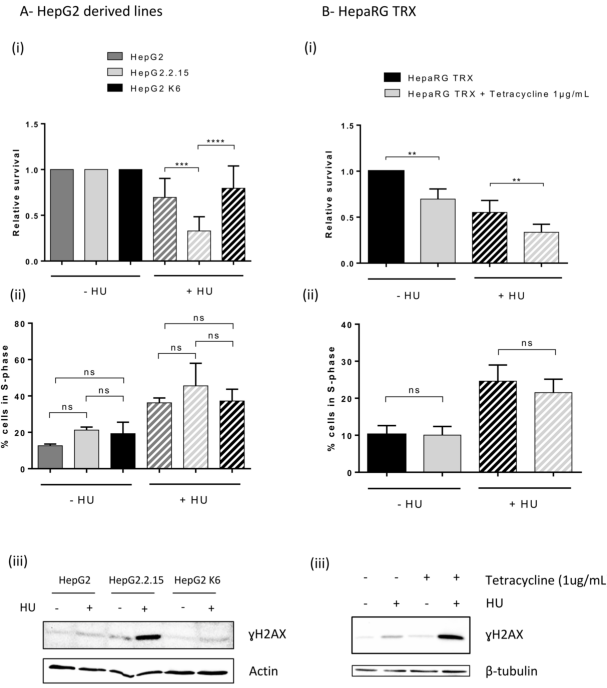
A- HepG2 derived lines
B- HepaRG TRX
(i)
HepG2
HepG2.2.15
HepG2 K6
Relative survival
1.5
1.0
0.5
0.0
***
****
- HU
+ HU
HepaRG TRX
HepaRG TRX + Tetracycline 1µg/mL
**
**
(ii)
% cells in S-phase
80
60
40
20
0
ns
- HU
+ HU
40
30
20
10
0
(iii)
HepG2
HepG2.2.15
HepG2 K6
HU
γH2AX
Actin
Tetracycline (1ug/mL)
β-tubulin

Figure 4

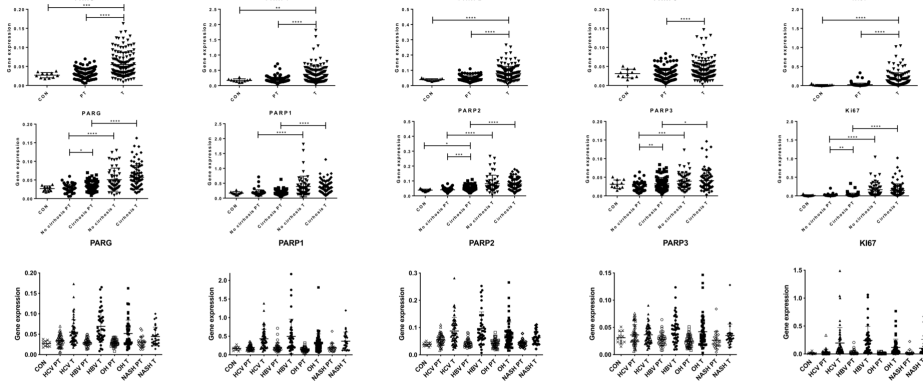

CON vs	Genes				
	PARG	PARP1	PARP2	PARP3	KI67
HCV PT	ns	ns	*	ns	*
HBV PT	ns	ns	ns	ns	ns
OH PT	ns	ns	ns	ns	ns
NASH PT	ns	ns	ns	ns	ns

PT vs	Genes				
	PARG	PARP1	PARP2	PARP3	KI67
HCV T	***	****	**	ns	****
HBV T	****	****	****	***	****
OH T	***	****	***	**	****
NASH T	ns	*	**	ns	***

Figure 5

A

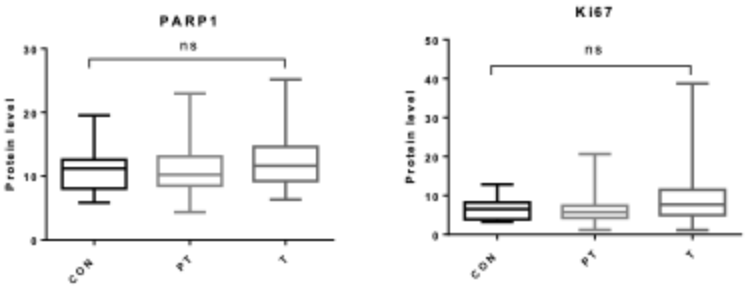
PARP1
ns
Protein level
30
20
10
0
CON
PT
T
Ki67
ns
Protein level
50
40
30
20
10
0
CON
PT
T

B

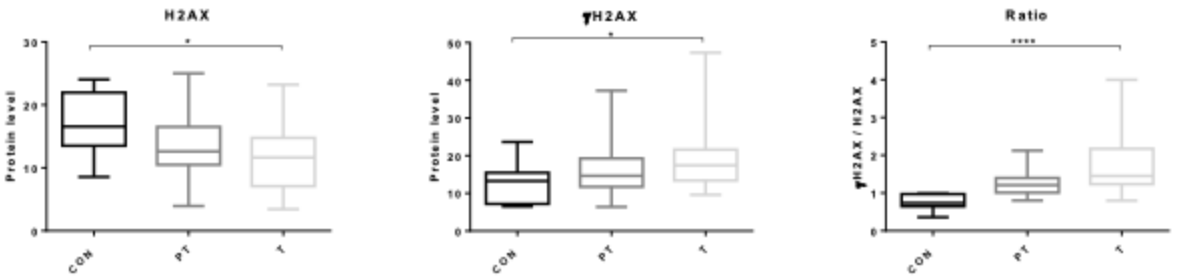
H2AX
*
Protein level
30
20
10
0
CON
PT
T
γH2AX
*
Protein level
50
40
30
20
10
0
CON
PT
T
Ratio
****
γH2AX / H2AX
5
4
3
2
1
0
CON
PT
T